THE JOURNAL OF PHYSICAL CHEMISTRY B

Article

pubs.acs.org/JPCB

Correlating Infrared and X-ray Absorption Energies for Molecular-Level Insight into Hydrogen Bond Making and Breaking in Solution

Mirabelle Prémont-Schwarz,[†] Simon Schreck,[‡,∥] Marcella Iannuzzi,[§] Erik T. J. Nibbering,*[,†] Michael Odelius,*[,#,∥] and Philippe Wernet*[,‡]

[†]Max-Born-Institut für Nichtlineare Optik und Kurzzeitspektroskopie, Max-Born-Strasse 2 A, 12489 Berlin, Germany

[‡]Institute for Methods and Instrumentation for Synchrotron Radiation Research, Helmholtz-Zentrum Berlin für Materialien und Energie GmbH, Albert-Einstein-Strasse 15, 12489 Berlin, Germany

[∥]Institut für Physik und Astronomie, Universität Potsdam, Karl-Liebknecht-Strasse 24-25, 14476 Potsdam, Germany

[§]Institute of Physical Chemistry, University of Zurich, Winterthurerstrasse 190, CH-8057 Zurich, Switzerland

[#]Department of Physics, Stockholm University, AlbaNova University Center, 106 91 Stockholm, Sweden

Supporting Information

ABSTRACT: While ubiquitous, the making and breaking of hydrogen bonds in solution is notoriously difficult to study due to the associated complex changes of nuclear and electronic structures. With the aim to reduce the according uncertainty in correlating experimental observables and hydrogen-bond configurations, we combine the information from proximate methods to study the N−H···O hydrogen bond in solution. We investigate hydrogen-bonding of the N−H group of *N*-methylaniline with oxygen from liquid DMSO and acetone with infrared spectra in the N−H stretching region and X-ray absorption spectra at the N K-edge. We experimentally observe blue shifts of the infrared stretching band and an X-ray absorption pre-edge peak when going from DMSO to acetone. With ab initio molecular dynamics simulations and calculated spectra, we qualitatively reproduce the experimental observables but we do not reach quantitative agreement with experiment. The infrared spectra support the notion of weakening the N−H···O hydrogen bond from DMSO to acetone. However, we fail to theoretically reproduce the measured shift of the X-ray absorption pre-edge peak. We discuss possible shortcomings of the simulation models and spectrum calculations. Common features and distinct differences with the O−H···O hydrogen bond are highlighted, and the implications for monitoring hydrogen-bond breaking in solution are discussed.

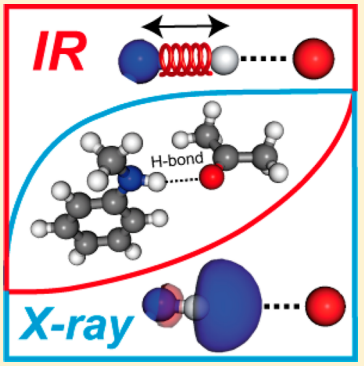

INTRODUCTION

Hydrogen bonding plays a key role in the interaction between protic solvent molecules such as water and determines the structure of nucleic acid base pairs such as DNA.[1−4] Midinfrared (IR) spectroscopy has a long-standing history as a local probe for studying hydrogen-bond interactions and switching.[5−16] It is well established that the O−H and N−H stretching vibrations are sensitive marker modes for identifying and characterizing hydrogen bonded complexes as they can be typified by the pronounced frequency red-shift, line broadening, and increase in absorption cross section of the stretch vibration compared to those of the free, uncomplexed O−H or N−H groups. However, in contrast to structurally well-ordered inorganic and molecular crystals, a direct correlation between hydrogen stretching frequency shift and hydrogen-bond strength cannot a priori be made. Instead, the influence of the polarizing surrounding solvent has to be determined for each individual case, which, for solution-phase samples, is an ongoing topic of research.[17−21] This motivates developing and testing alternative or complementary methods for studying hydrogen-bond interactions in solution. Given the fact that both nuclear and electronic degrees of freedom change upon hydrogen bonding it is in particular the access to the electronic structure changes that motivates corresponding approaches. Combining knowledge of nuclear and electronic-structure changes upon hydrogen bonding, finally, promises for an in-depth understanding of hydrogen-bond switching.

X-ray absorption spectroscopy (XAS), also known as near-edge X-ray absorption fine structure spectroscopy (NEXAFS)[22] at the O and N K-edges has proven to be a useful tool in studying hydrogen-bonding. It was used in particular for the investigation of extended hydrogen-bond networks and their dynamics,[23−31] tautomerism of intramolecular hydrogen bonds[32] and dimerization in solution by hydrogen-bonding,[33] hydrogen bonding in amino acids[34−36] and DNA,[37] and hydrogen-bonding of aromatic molecules in solution[38] and for elucidating the interactions of proteins with salts and the Hofmeister effect.[39]

The O or N K-edge absorption bands arise from transitions of O or N core−shell 1s electrons into empty molecular

Received: March 27, 2015
Revised: May 29, 2015
Published: June 1, 2015

DOI: 10.1021/acs.jpcb.5b02954
J. Phys. Chem. B 2015, 119, 8115−8124

orbitals. Due to the dipole selection rule their amount of p-character is probed. The O and N 2p orbitals are directly involved in bonding of R−O−H or R−N−H, and as hydrogen-bonding alters this bonding, K-edge XAS is directly sensitive to the O−H···X[26] and N−H···X hydrogen-bonding interactions. On one hand, while the molecular-orbital interactions upon hydrogen bonding can be revealed with XAS, it lacks direct structural information. On the other hand, IR spectroscopy gives access to structural degrees of freedom, but it is limited in terms of electronic-structure information.

The aim here is to combine the information from IR and X-ray absorption spectroscopy for a well-defined case of hydrogen-bonding in solution, namely the N−H···O hydrogen bond, to reduce the respective uncertainties, and to correlate experimental observables with hydrogen-bonding interactions. We present experimental and calculated results on hydrogen-bonding of the prototypical organic molecule *N*-methylaniline (NMA) in dimethyl sulfoxide (DMSO) and acetone solution. The choice of NMA with only one hydrogen-bonded N−H group reflects our utmost aim to simplify the problem to unambiguously identify fundamental correlations of IR stretching frequencies and X-ray absorption energies with hydrogen bonding interactions. In particular, due the presence of the methyl group, NMA has only one N−H stretching mode that is affected by hydrogen bonding. This considerably simplifies the IR spectrum and facilitates interpretation in terms of hydrogen-bond strength. Indeed, for an NH_2 group, additional excitonic couplings and a Fermi resonance of the N−H stretching $\nu = 1$ levels with the N−H bending $\delta = 2$ overtone state, as well as the symmetric and asymmetric stretching normal modes, would need to be considered.[40] The choice of solvents also reflects our desire to establish a simple model system. DMSO is a solvent with a strong hydrogen-bond interaction with NMA, while acetone makes a weaker hydrogen-bond. However, because both solvent molecules have the same symmetry, it considerably simplifies the ensuing calculations and allows us to focus on the strength of the specific interaction. Our results could help to understand more complex cases of hydrogen-bonding such as for water in acetonitrile[41,42] and DMSO[43] or for the NH_2 group of glycine[36] and the NH_3 group in alanine and sarcosine.[44] We aimed at typifying the expected trends in hydrogen-bond strength with strong hydrogen bonding to DMSO and weak hydrogen bonding to acetone by comparing N−H stretching IR and N K-edge X-ray absorption spectroscopic features of NMA. The experimental data are complemented by Car−Parrinello ab initio molecular dynamics (MD) simulations and spectrum calculations to explain the hydrogen-bonding interactions on a molecular level by addressing the orbital interactions. Surprisingly, we fail to reach quantitative agreement between theory and experiment even for this comparably simple system. We discuss the possibilities of either incorrectly simulating structures and hydrogen-bond configurations or incorrectly describing part of the X-ray transitions. Common features and distinct differences with the O−H···O hydrogen bond are highlighted, and the significance of the results for monitoring hydrogen-bond breaking in solution are discussed.

METHODS

Reagents. *N*-Methylaniline [Fluka, purum, ≥98.0% (GC)], dimethyl sulfoxide (Acros Organics, 99.7+%, extra dry over molecular sieves, AcroSeal), acetone (Sigma-Aldrich, ACS spectrophotometric grade, ≥99.5%), and cyclohexane (see Supporting Information, Sigma-Aldrich, laboratory reagent, ≥99.8%) were used as received.

FT-IR Measurements. Measurements were performed using a FT-IR Varian 640-IR spectrometer. Spectra were measured on solutions with a concentration of *N*-methylaniline in DMSO and acetone of 20 mM. The solutions were placed in a cell made of $CaCl_2$ windows separated by 50 μm Teflon spacers. In cyclohexane (see Supporting Information), an 8 mM concentration was used with a 250 μm path length. We measured IR spectra at various concentrations in the solvents used in this study. We have only shown IR spectra of NMA in cyclohexane, DMSO, and acetone at the lower concentration of 20 mM; however, we also did a concentration-dependent series of IR spectra of NMA. In particular, at concentrations of 0.2 M and higher, self-association was observed, but only in nonpolar solvents like cyclohexane or C_2Cl_4, as evidenced by a shoulder around 3425 cm^{-1}, whereas in acetone or DMSO these features were not observed. Even then, the amount of self-association is still of small magnitude, as the main portion of the N−H stretching band reflects the monomer contribution. Self-association of anilines has been estimated to be less than 10% at a total concentration of 0.3 M in cyclohexane solution.[45] Noting that the hydrogen bonding propensity of aniline is higher than that of *N*-methylaniline, we conclude that self-association, predominantly driven by hydrogen bonding, is of minor importance even in nonpolar cyclohexane solution. Accordingly, self-association of NMA in acetone or DMSO solution will even be less important.

NEXAFS Measurements. Samples of 0.3 M *N*-methylaniline were prepared and thoroughly degassed under vacuum. A sample holder with X-ray-transparent silicon nitride membranes allowing for the reliable preparation of ultrathin liquid films with an adjustable thickness in the nanometer to micrometer range was used for the NEXAFS measurements. A more detailed description of the experimental setup are reported in refs 46 and 47. Measurements were carried out at the UE56-1_PGM beamline at Helmholtz-Zentrum Berlin. NEXAFS spectra were measured using 3 to 5 μm thin liquid films by detecting the transmitted X-ray flux with a photodiode. The incident photon flux was adjusted to 10^7 photons/s by detuning the undulator gap. This ensures that no radiation damage or instabilities of the sample are induced by the X-rays. The bandwidth of the incident photon beam and thus the spectral resolution was 200 meV.

Theoretical Calculations. Car−Parrinello MD simulations[48] were performed for a single *N*-methylaniline molecule solvated by 40 solvent molecules in cubic simulation cells with periodic boundary conditions. The ab initio MD simulations were initialized from classical MD simulations at ambient temperature and pressure in the NPT ensemble with MDynaMix[49] using the Amber force field[50] for NMA. To obtain reasonable initial solvation conditions for the ab initio MD simulations, the partial point charges in the classical force field were fitted to the electrostatic potential obtained from density functional calculations of the *N*-methylaniline molecule in a polarizable continuum at the B3LYP/aug-cc-pVTZ level in Gaussian 09.[51−53] For DMSO and acetone, the Geerke et al.[54] and OPSLAA[55] force fields were employed in the classical simulations. The classical MD simulations resulted in mean cell lengths of 16.9511 Å in DMSO and 17.2618 Å in acetone. These were employed in the ab initio simulations performed with the CPMD program.[56]

DOI: 10.1021/acs.jpcb.5b02954
J. Phys. Chem. B 2015, 119, 8115−8124

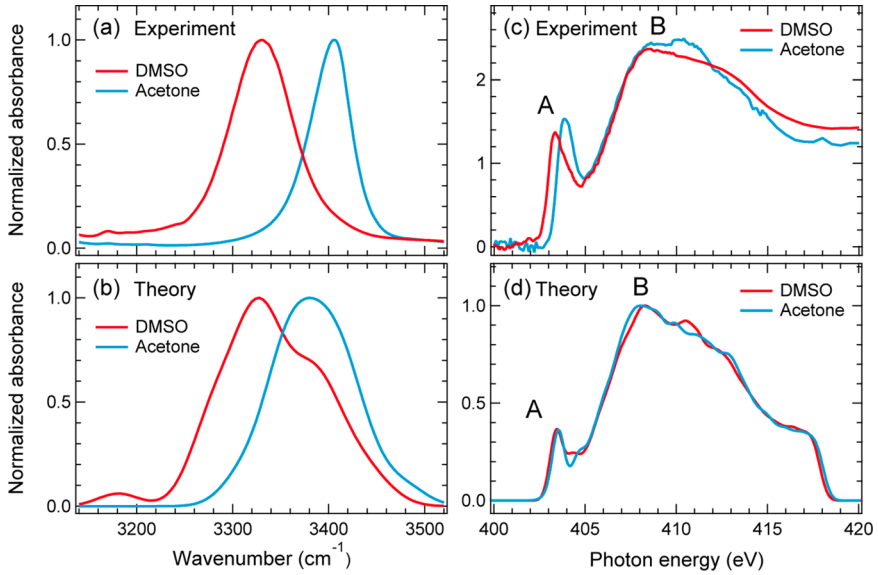

Figure 1. Measured and calculated infrared and X-ray absorption spectra of *N*-methylaniline (NMA) in liquid DMSO and acetone. (a and b) Measured and calculated infrared absorption spectra in the N−H stretching region. (c and d) Measured and calculated X-ray absorption spectra at the N K-edge. The infrared spectra are normalized to 1 at maximum. The measured X-ray absorption spectra are normalized to 1 at the edge jump (at 430 eV). The theoretical X-ray absorption spectra are displayed as calculated.

The systems were deuterated, and a fictitious energy mass of 800 au was combined with a time-step of 6 au in a Car−Parrinello MD simulation[48,56] which were equilibrated for 15 ps and then sampled for 13 ps. The electronic structure was described with density functional theory with a gradient corrected functional (BLYP) complemented with van der Waals interactions to obtain an accurate description of both the polar and nonpolar groups.[57−59] Pseudopotentials of Trouillier−Martins type[60] were used in combination with a 70 Ry kinetic energy cutoff for the plane wave expansion of the Kohn−Sham wave functions. For hydrogen, however, a local pseudopotential parametrized with one Gaussian was used. The pseudopotentials were expressed in the Kleinman−Bylander form[61] and were local in the highest angular momentum ($l = 2$ for sulfur and $l = 1$ for C, N, and O).

The nitrogen K-edge X-ray absorption spectra of *N*-methylaniline solvated in DMSO and acetone solutions was calculated using the half-core hole transition potential method as implemented in the fully periodic framework in CP2K[62−65] with a combination of an all-electron description of the core-excited atom and pseudopotentials on the remaining atoms. To compare with the experimental data, the discrete spectra were convoluted with a Gaussian of 0.6 eV fwhm and averaged over many configurations, and an ad-hoc constant energy shift of +0.3 eV was applied to the CP2K results. The CP2K calculation of isolated NMA was performed in a cubic simulation cell with a 30 Å cell dimension and a poison solver for nonperiodic systems. The IR spectra for solvated NMA in DMSO and acetone were derived from cluster calculations in Gaussian 09,[51] in which, for each sampled configuration, a partial (freezing all other atoms in the cluster) optimization and subsequent vibrational analysis of the N−H group in NMA was performed. We employed the gradient-corrected B3LYP functional and a triple-ζ basis set.[52,66] The IR spectra were represented as the distribution of discrete frequencies weighted with their IR intensities. For the calculated IR frequencies, a constant shift of -168.3 cm^{-1} was applied for alignment of the calculation of the isolated NMA molecules with the experimental data for the cyclohexane solution, presented in Figure S1, Supporting Information. This shift is intended to account for both anharmonicity, lacking in the calculated harmonic frequencies, and limitations of the DFT functional.

RESULTS

The measured and calculated N−H stretching IR and N K-edge X-ray absorption spectra of NMA in DMSO and acetone are depicted in Figure 1. The most noticeable effects in the experimental spectra are the blue shifts in both the IR spectra (Figure 1a) and the pre-edge peak at around 403 eV in the X-ray absorption spectra (Figure 1c) when going from DMSO to acetone. The IR stretching band shifts by 75 cm^{-1} and the XAS pre-edge shifts by 0.5 eV. The IR blue shift suggests a weakening of the hydrogen-bond interactions when going from DMSO to acetone. It is reproduced in the calculated IR spectra in Figure 1b, but the magnitude of the shift is somewhat underestimated (50 cm^{-1} compared to the measured 75 cm^{-1}). Notice that while we employed deuteration in the MD simulations to ensure stability in the Car−Parrinello algorithm, the IR spectrum simulations on sampled clusters were performed without deuteration. The calculated IR spectra are too broad in comparison to experiment. Extended investigations on prolonged MD simulations are planned for the future to study in more detail the IR and X-ray absorption spectra for specific classes of H-bonding environment. The overall shape of the N K-edge absorption spectrum with a pronounced pre-edge peak at around 403 eV is theoretically reproduced by our spectrum calculations (Figure 1d), but the calculated blue shift of 0.1 eV is much smaller than the experimentally observed shift of 0.5 eV. It is the aim of the following discussion to elucidate the correlation of IR and X-ray absorption peak shifts with hydrogen-bond strengths and to find possible reasons for the failure of our theoretical description of the investigated systems.

DOI: 10.1021/acs.jpcb.5b02954
J. Phys. Chem. B 2015, 119, 8115−8124

DISCUSSION

The N−H stretching bands of NMA are red-shifted in both the hydrogen-bond accepting solvents DMSO (3330 cm^{-1}) and acetone (3405 cm^{-1}) with respect to NMA in the non-hydrogen-bonding solvent cyclohexane (3442 cm^{-1}) (see Figure S1, Supporting Information). Also, IR line broadening decreases from 75 cm^{-1} in DMSO to 50 cm^{-1} in acetone (and to 20 cm^{-1} in cyclohexane, full width at half maximum). Furthermore, the IR absorption cross section decreases from 111 M^{-1} cm^{-1} in DMSO to 83 M^{-1} cm^{-1} in acetone (and to 35 M^{-1} cm^{-1} in cyclohexane).[67] Such features are indicative of decreasing solute−solvent couplings and weakening of the N−H···O hydrogen-bond interactions between the solute N−H group and the solvent O atom when going from DMSO to acetone. Using the semiempirical correlation of hydrogen-stretching frequencies with hydrogen-bond distances as measured with X-ray or neutron diffraction,[6] we estimate a decrease in the average hydrogen-bonding N···O distances on the order of 0.5−1 Å when dissolving NMA in DMSO compared to acetone. However, it is well-known that this hydrogen stretching frequency−structure correlation based on data from inorganic crystals is of limited use, and it becomes even more blurred for hydrogen-bonded systems in liquid solution.[17,18,14] In particular the role of nonspecific solute−solvent interactions compared to specific hydrogen bonding and their respective influences of the stretching frequencies remains unclear.

To shed light on this, we performed ab initio MD simulations of NMA in DMSO and acetone. The extracted radial distribution functions (RDFs) are displayed with structural models for the hydrogen-bonded complexes in Figure 2. The RDFs clearly indicate that the average hydrogen-bonding N···O distances in N−H···O (see models in Figure 2 a,b) increase when going from NMA in DMSO (2.96 Å) to acetone (3.1 Å) (see the positions of the maxima of the first peaks in $g_{NO}(r)$ in Figure 2c). Correspondingly, the calculated hydrogen-bond H···O distances are smaller for NMA in DMSO (1.99 Å) compared to acetone (2.11 Å) (see the positions of the maxima of the first peaks in $g_{HO}(r)$ in Figure 2d). Our simulations show no significant difference in the intramolecular N−H distance upon decreasing hydrogen-bonding interactions from DMSO to acetone. Our simulated structures thus qualitatively support the notion derived from the IR data of stronger (shorter) N−H···O hydrogen bonds of NMA in DMSO compared to acetone. However, the calculated decrease of 0.14 Å in the N···O distance upon hydrogen-bond strengthening are about five times smaller than the decrease estimated above with the semiempirical correlation of IR hydrogen-stretching frequencies with hydrogen-bond distances. The question arises whether this is due to an ambiguous correlation between stretching frequency shift and hydrogen-bond strength or instead to deficiencies in simulating the solute−solvent structures. To investigate the simulation model, the ab initio simulations will be further pursued in a subsequent study, but preliminary results from simulations, in which the densities of the solutions are relaxed at constant pressure, confirm that the difference in N−H···O hydrogen bond lengths is smaller than expected from the semiempirical correlation in IR spectroscopy. We also notice that there is a weak interaction between the methyl groups and the amine group, which is more pronounced in DMSO than in acetone (RDFs not shown). However, because the corresponding H···N distance is long

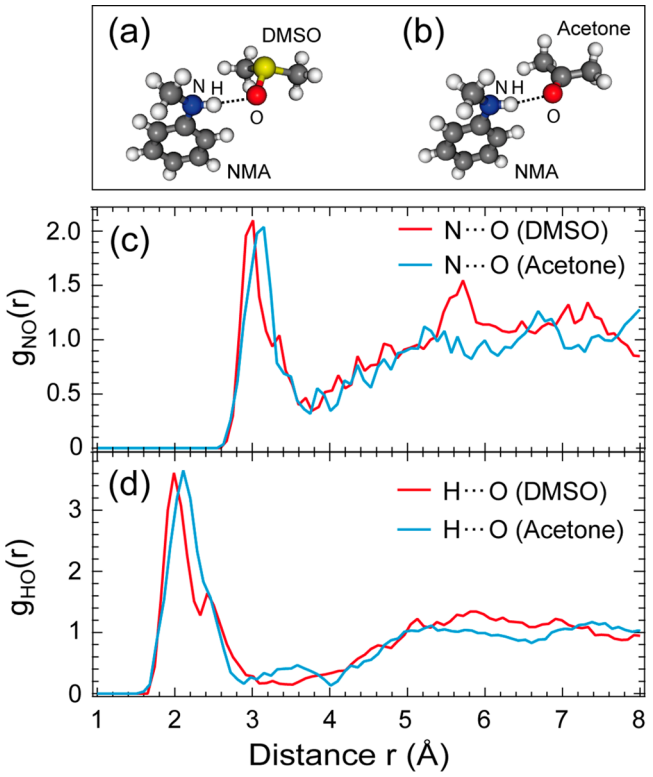

Figure 2. Structural models of (a) the *N*-methylaniline−DMSO (NMA−DMSO) and (b) the NMA−acetone complexes. N−H···O hydrogen bonds are indicated as dashed lines. (c and d) Radial distribution functions of the solvation structure around the amino group of NMA in DMSO and acetone as deduced from ab initio MD simulations (c: N···O distances, and d: H···O distances).

(around 3.0 Å), we have no indication that it influences the IR or X-ray spectra.

We now consider the nature of the blue shift of the pre-edge in the N K-edge X-ray absorption spectrum (Figure 1c) and see whether it can be used to delimit possible changes in hydrogen-bond interactions as derived from the IR spectra. The underlying idea is based on the knowledge acquired from O K-edge X-ray absorption spectra of the O−H···O hydrogen bond.[25−29] There, it could be established that the pre-edge peak at around 535 eV is dominated by transitions from the 1s core level to antibonding σ orbitals oriented along the O−H bond and arising from hybridization of the O 2s and 2p orbitals. It was found that the weaker the hydrogen bond, the smaller the s and the larger the p contributions, explaining, due to the dipole selection rule, the stronger pre-edge intensity for weaker hydrogen bonds.

To assign the pre-edge peak in the N K-edge X-ray absorption spectrum of NMA in DMSO and acetone, we first analyze the calculated N K-edge X-ray absorption spectrum of isolated or uncomplexed NMA with the aid of Figure 3 and with the orbital plots shown in Figure 3a−c. We find that the pre-edge peak for uncomplexed NMA, located at 404.3 eV (Figure 3d, total cross section), arises from two strong X-ray transitions of the 1s core electron to the LUMO+1 and the LUMO+2 orbitals. The decomposition of the calculated total cross section into the mutually perpendicular directions *x*, *y*, and *z* according to the molecular coordinate system in Figure 3c allows for assigning these transitions. In the sampling over the MD simulations, the XAS transition moments were

DOI: 10.1021/acs.jpcb.5b02954
J. Phys. Chem. B 2015, 119, 8115−8124

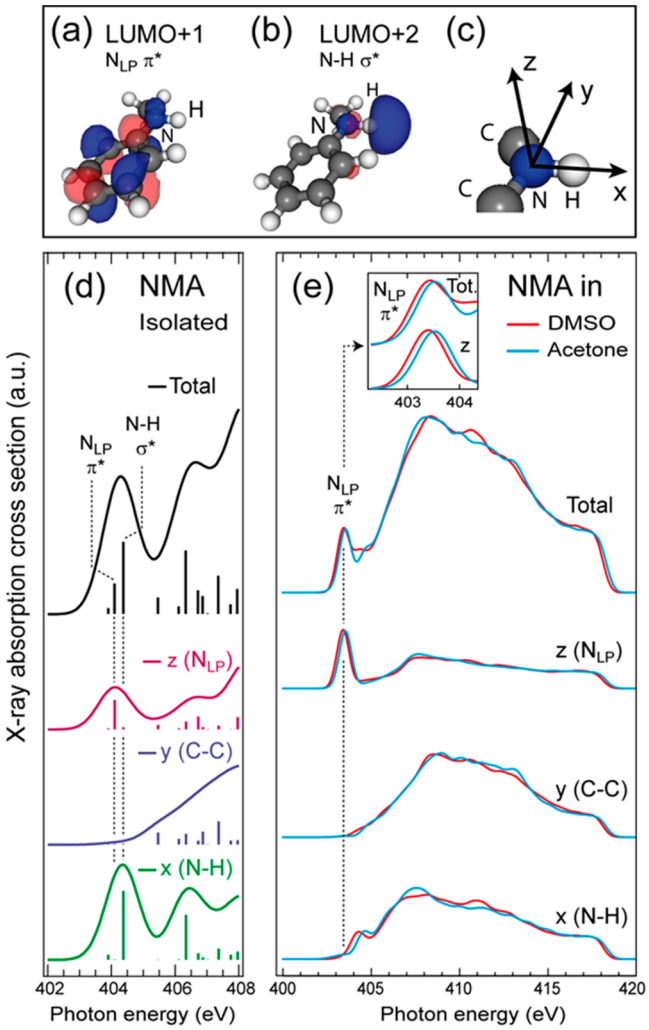

Figure 3. Orbital plots of (a) the LUMO+1 (N π*lone pair, N_{LP} π*) and (b) the LUMO+2 (σ* oriented along the N−H bond, N−H σ*) in isolated *N*-methylaniline (NMA) (isosurfaces corresponding to an amplitude of 0.05 of the normalized orbitals are plotted with the approximated core hole on the N). (c) Definition of the coordinate system with *x* along the N−H bond, *y* along the C−C axis, and *z* perpendicular to the *x*−*y* plane. (d) Calculated N K-edge absorption spectrum of isolated NMA with total cross section (black) and decomposed into the *x*, *y*, and *z* directions (intensities of the individual transitions are represented by sticks). The dashed line at 404.1 eV (404.4 eV) denoted N_{LP} π* (N−H σ*) marks the absorption maximum for transition into the N lone pair π* orbital (transition into the σ* orbital along the N−H bond). (e) Calculated N K-edge absorption spectra of NMA in DMSO and acetone with total cross section (top) and decomposed into the *x*, *y*, and *z* directions.

transformed to the molecular coordinates systems before averaging. The *z* component (direction of the N lone pair orbital) solely contributes to the LUMO+1 excitation. As it arises from transitions into the N lone pair orbital with antibonding π* character (N_{LP} π*, Figure 3a), the LUMO+1 transition can be assigned to N_{LP} π* excitations. The *x* component (direction of the N−H bond) dominates the LUMO+2 transition, which can be thus assigned to the corresponding N−H σ* transitions arising from excitations into the antibonding σ* orbital that is oriented along the N−H bond (N−H σ*, Figure 3b). This is in agreement with the assignments of the N K-pre-edge transitions in gaseous pyrrole, which has a similar geometric and electronic structure around the N−H group as NMA, as measured with XAS[68] and inner-shell electron energy loss spectroscopy.[69]

To investigate the solvent effect, the calculated total cross sections and their decompositions into *x*, *y*, and *z* are plotted for NMA in DMSO and acetone in Figure 3e. One sees that, in contrast to the uncomplexed case, the N−H σ* transition is quenched or strongly reduced and shifted into the main absorption edge in both solutions [compare the *x* (N−H) components in Figure 3e and 3d]. In accordance with the discussion above on the O K-edge absorption spectrum of O−H···O hydrogen bonds, this can be explained by the fact that the hybridization of the N 2s and 2p orbitals in the N−H σ* orbital is strongly affected by hydrogen bonding in the sense that the amount of s character is increased at the detriment of p character due to coordination of the free N−H group with the O accepting lone air orbitals of the solvent molecules. N K-edge XAS probes the amount of p character in the unoccupied orbitals, and this explains the quenching of the N−H σ* excitations upon coordination of the N−H group.

Surprisingly, the N−H σ* orbital of NMA in both DMSO and acetone is quenched and the pre-edge peaks in the corresponding N K-edge absorption spectra are thus solely due to N_{LP} π* transitions as evidenced by the *z* (N_{LP}) component in Figure 3e. As a consequence, the measured blue shift of the pre-edge peak upon weakening the hydrogen-bond can be assigned to an increase of the corresponding N_{LP} π* transition energy (see the inset in Figure 3e). We note, however, that our calculations with a shift of 0.1 eV fail to reproduce the large measured shift of 0.5 eV.

Due to this disagreement of calculated and measured X-ray absorption pre-edge shifts and the inconsistency of the calculated H-bond lengths compared to the expectations from the semiempirical correlation of IR frequencies with hydrogen-bond distances, we need to question whether our theoretical treatment of the hydrogen-bonding interactions and the corresponding description of the experimental observables is correct.

To test this, we consider in the following H-bond switching events in our MD simulations. This allows us to study the evolution of our set of correlated observables of IR frequencies, X-ray absorption energies, and atomic distances for continuously varying H-bond length (strengths).

The N−H···O hydrogen-bond exchange dynamics of NMA in DMSO and acetone is monitored over a period of 15 ps with the sequences of MD simulations plotted in Figure 4. Hydrogen-bond switching events are present at around 6 ps for DMSO and at 7 ps for acetone. The ab initio MD simulations cover a too short time period to appropriately discuss the exchange time, but they allow us to characterize the hydrogen-bond exchange mechanisms. Even though NMA is comparably small, the motion of its N−H group are expected to be constrained by the aromatic ring acting as a molecular "backbone", which moves on a much longer time-scale. Correspondingly, we find comparably long hydrogen-bond exchange events that appear to be governed by the dynamics of the solvent molecules. Around the exchange events, there are periods when the system seems to explore various options of hydrogen bonding before the process is fully completed after around 8 ps for DMSO and 3 ps for acetone. Accordingly, in DMSO a few unsuccessful events are clearly observed [see the out-of-phase oscillations of DMSO solvent molecules leaving

DOI: 10.1021/acs.jpcb.5b02954
J. Phys. Chem. B 2015, 119, 8115−8124

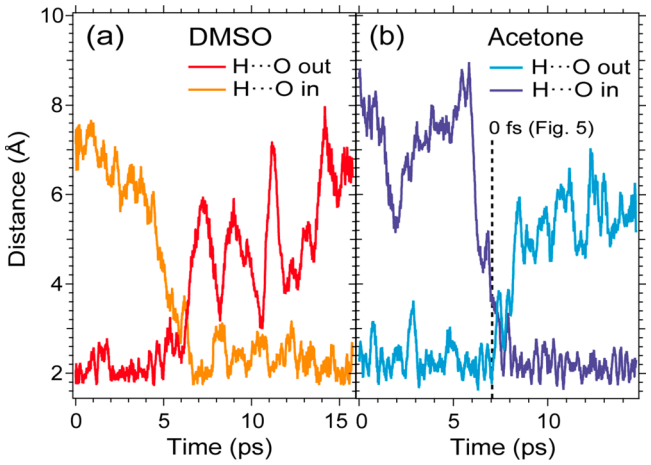

Figure 4. Hydrogen bond switching dynamics as quantified by the H···O distances in N−H···O of *N*-methylaniline (NMA) in (a) DMSO and (b) acetone and as derived from the ab initio MD simulations. "Out" and "in" denote the DMSO and acetone solvent molecules leaving (out) and entering (in) the solvation complex associated with hydrogen-bond breaking and formation, respectively. The dashed line in b marks time zero for the hydrogen-bond breaking event depicted in more detail in Figure 5.

(out) and entering (in) the solvation complex with extrema at 7, 9, and 11 ps in Figure 4a].

In contrast to the O−H groups in water molecules, which undergo large amplitude fluctuations,[10,70] the N−H bond in NMA is predominantly in an intact hydrogen-bond configuration. This is corroborated by the IR spectra in Figure 1, which exhibits a single red-shifted line in both acetone and DMSO, and it explains the different hydrogen-bond dynamics compared to O−H groups in water. In aqueous solution,[10,70] the water molecules easily reorient and the hydrogen-bond exchange of O−H involves ultrafast large-amplitude orientational jumps, which, coupled to the solvation dynamics, result in a faster hydrogen-bond switching on the time-scale of 1 ps.

With the calculated X-ray absorption spectra and normal-mode frequencies for the N−H stretch vibration in Figure 5, we follow the changes of the X-ray absorption energies and IR frequencies correlated with hydrogen-bond exchange by zooming into the femtosecond dynamics immediately around the switching process in the exemplary case of NMA in acetone.

As expected from our previous results, we find that the N K-pre-edge peak and the IR frequencies blue shift upon weakening or breaking of the N−H···O hydrogen bond. After 230 fs, the N K-pre-edge peak shift amounts to approximately 0.5 eV and the IR frequency shift amounts to 76 cm^{-1}. The corresponding elongation of the H···O distance is 1.1 Å (compare the structural snapshots in Figure 5b with an H···O distance elongation from 2.0 to 3.1 Å where 2.0 Å correspond to the intact hydrogen bond, see Figure 2d). The calculated elongation of the hydrogen-bond distance thus corresponds to the expected elongation by 0.5−1 Å for an IR frequency shift of 76 cm^{-1} as based on the semiempirical correlation of hydrogen-stretching frequencies with hydrogen-bond distances. The calculated XAS pre-edge and IR frequency shifts of 0.5 eV and 76 cm^{-1} perfectly fit to the measured shifts of 0.5 eV and 75 cm^{-1} when going from NMA in DMSO to NMA in acetone. However, the calculated H···O distance change of only 0.12 Å when going from NMA in DMSO to NMA in acetone is at odds with this. We thus find that either our structural models

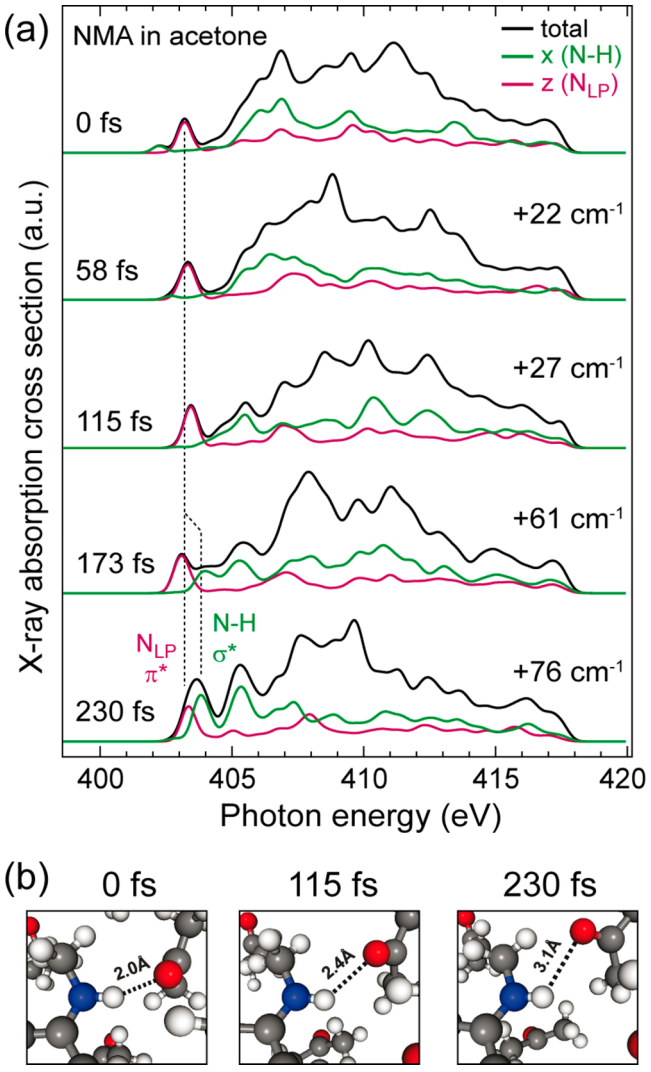

Figure 5. (a) Time evolution of the calculated N K-edge absorption spectrum of *N*-methylaniline (NMA) in acetone during an N−H···O(acetone) hydrogen bond breaking event (extracted from the full ab initio MD simulations at ∼7 ps, see Figure 4b) with total cross section (black) and *x* (along N−H bond) and *z* (along the N lone pair) components (definition of coordinate system in Figure 3). The dashed line at 403.5 eV denotes the absorption maximum of the N_{LP} π^* peak (transition into the N lone pair π^* orbital) at 0 fs. The line at 403.9 eV marks the maximum of the N−H σ^* peak (transition into the σ^* orbital along the N−H bond). Calculated changes of the vibration normal-mode frequencies for the N−H stretch vibration are given with respect to 0 fs. (b) Zoomed-in views of the N−H···O(acetone) hydrogen-bond configurations at 0, 115, and 230 fs from the ab initio MD simulations with indicated hydrogen-bond length (H···O distances, dashed lines).

for NMA in DMSO and acetone are incorrect in terms of exhibiting too little change in hydrogen bond interactions when going from DMSO to acetone, or other factors affect the observables that cannot be related directly to changes in the hydrogen-bond interactions or in the hydrogen-bond strength. To shed further light on this, we analyze in more detail the temporal evolution of the calculated XAS pre-edge peak separately for the N_{LP} π^* and for the N−H σ^* components and compare these to the calculated IR frequency shifts in Figure 5.

DOI: 10.1021/acs.jpcb.5b02954
J. Phys. Chem. B 2015, 119, 8115−8124

Strikingly, the XAS pre-edge peak blue shifts from 0 to 58 fs and from 58 to 115 fs but it shifts back approximately to its original position at 173 fs and blue shifts again at 230 fs. The IR frequencies in contrast continuously blue shift throughout the hydrogen-bond switching process. At 115 fs (H···O distance 2.4 Å), the XAS pre-edge shift is primarily due to a blue shift of the N_{LP} π^* transition, as up to this point the N−H σ^* transition is still quenched by remaining hydrogen-bonding interactions [see the calculated z (N_{LP}) component in Figure 5a]. This dynamic N_{LP} π^* shift amounts to approximately 0.2 eV (H···O distance change 0.4 Å), thus being smaller than the shift extrapolated from the calculated steady-state N_{LP} π^* shift of 0.18 eV for an H···O distance change 0.12 Å of NMA in DMSO compared to acetone. At 173 fs, the N_{LP} π^* transitions momentarily undergo a red shift with the N−H σ^* peak increasing at higher energies. At 230 fs, the overall pre-edge peak has further shifted to higher energies but this is now due to the combined effect of the upcoming N−H σ^* peak and the again blue-shifting N_{LP} π^* transition. Note that at 230 fs, the acetone solvent molecule has left the complex and the incoming acetone molecule has not reached bonding distance [compare H···O "out" and "in" in Figure 4b shortly after the dashed line]. Accordingly, and in agreement with our findings discussed with Figure 3, the N−H σ^* transition is a clear manifestation of the broken H-bond.

This complex interplay of shifting N_{LP} π^* and N−H σ^* components explains why the overall blue-shift of the N−K-pre-edge peak upon hydrogen-bond breaking cannot be extrapolated from the steady-state shift of NMA in DMSO and acetone. The dynamic blue-shift is due to the combined effect of N_{LP} π^* shift and upcoming N−H σ^* peak whereas the steady-state shift is solely due to the N_{LP} π^* shift. Hydrogen-bond breaking leads to a redistribution of spectral weight in the N−H σ * component with an additional shift of the N_{LP} π * component, both thereby contributing to the overall XAS pre-edge shift. Depending on the specific molecular configuration, the shift of the N_{LP} π^*can be in different directions.

While the N−H σ^* component thus reacts as expected to changes in hydrogen bond strength the N_{LP} π^* peaks seems to pick up structural changes that are not directly related to changes in the N−H···O hydrogen-bond interactions. This is novel information that can be easily overlooked when considering the continuous shift of the IR frequencies with breaking the hydrogen bond. Closer inspection of the simulated structure at 115 fs in Figure 5, where the N−H σ^* component is still quenched, indicates that bonding of N to the neighboring methyl group affects the N_{LP} π^* peak energy. We find that the calculated N_{LP} π^* blue shift of 0.2 eV correlates with a decrease in the *N*-methyl distance of 0.06 Å. This must still be related to weakening the hydrogen-bond, as the H···O distance in the N−H···O hydrogen-bond increases by 0.4 Å but rather than probing the hydrogen-bond interactions directly and exclusively we are also sensitive to changes in the *N*-methyl bond. In this sense, the steady-state shift of the XAS pre-edge peak of NMA in DMSO and acetone results from an ensemble average of a distribution of configurations with both different hydrogen bonding and varying *N*-methyl distances and hence varying N_{LP} π^* peak energies. Compared to isolated NMA, the calculated XAS pre-edge energy in NMA in both DMSO and acetone is red-shifted by approximately 1 eV upon solvation. Schwartz et al. found a redshift of the N K-pre-edge peak of 0.3 eV for pyrrole upon solvation in aqueous solution compared to the peak position in the X-ray absorption spectrum of pyrrole in the gas phase.[38] Their explanation, however, remained somewhat inconclusive in terms of a correlation with changes in the hydrogen-bond interactions. We speculate that this might, similar to our case with NMA in DMSO and acetone, be due to solvation of pyrrole that could be associated with a combined change of hydrogen-bond interactions and changes of the electronic structure due to changes in the overall molecular structure including atoms and groups of atoms not directly involved in the hydrogen bond. From the IR spectroscopy point of view, the latter can be related to electrostatic or polarization effects. Using a comparison of the N−H stretching frequency shifts of NMA hydrogen-bonded complexes in cyclohexane and in the neat solvents (DMSO and acetone) allows us to estimate the relative strength of these nonspecific interactions with respect to the magnitude of the specific hydrogen-bond interactions. For the hydrogen-bonded NMA−DMSO complex, we observe the N−H stretching band to be located at 3371 cm^{-1} in cyclohexane solution, whereas in DMSO solution it further red-shifts to 3330 cm^{-1}. For hydrogen-bonded NMA−acetone complexes, we find the N−H stretching band at 3415 cm^{-1}, whereas in acetone solution it further downshifts to 3405 cm^{-1}. Noting that uncomplexed NMA in cyclohexane has an N−H stretching band located at 3442 cm^{-1}, we estimate that for NMA in DMSO, 30−40% of the IR frequency downshift is due to the nonspecific interactions, while for NMA in acetone, this amounts to 20−30%. Similar relative magnitudes have been obtained in a solvent-dependent transient IR study of the O−H stretching mode of 2-naphthol−acetonitrile complexes.[71]

We are left with the finding that the overall calculated XAS pre-edge shift for NMA in DMSO compared to NMA in acetone is approximately five times smaller than the experimentally observed shift, and we close with a discussion of possible reasons for this where we see two alternative explanations for this discrepancy. First, the simulated structures or molecular configurations from our ab initio MD simulation could be too rigid. Possibly due to a neglect of quantum effects in the nuclear motions, because of limitations in the density functional, or because the chosen system size was too small, we could have generated structures with too little freedom in varying bond lengths. This could affect the calculated XAS pre-edge shift in two ways. It could mean that we have too little variation of *N*-methyl bond distances and hence too little N_{LP} π^* peak shift. It could also mean that the length of the hydrogen-bonds is underestimated and in turn the intensity of the N−H σ^* component is underestimated. The question arises why the calculated IR frequency shift based on the same structures agrees so much better with the IR experiment? This could be explained by the fact that the resident time in distorted configurations is small compared to the resident time in the less distorted ones. Assuming a time scale of IR spectroscopy larger than the resident time in distorted configurations, IR spectroscopy would thus primarily probe the electrostatic interactions in the less distorted configurations. On the other hand, because XAS is more sensitive to the distribution of instantaneous configurations than IR spectroscopy, the contribution due to the distorted configurations would still be small but more pronounced in XAS than in IR spectroscopy. Thus, using structures which are too rigid, the calculated XAS pre-edge shift would turn out to be too small.

Our second and alternative explanation would be that we incorrectly treat the N−H σ^* component in the calculated spectrum. Within the employed half-core hole approximation, it

DOI: 10.1021/acs.jpcb.5b02954
J. Phys. Chem. B 2015, 119, 8115−8124

could be that the structural distortion or elongation of the hydrogen bond needed to generate an appreciable N−H σ^* peak intensity is too large compared to the distortion needed to generate an appreciable IR frequency shift. For the presumably correctly simulated structures, the calculated IR frequency shift would thus fit the experiment while the calculated N K-pre-edge peak shift would be too small. Alternatively, it could be that we incorrectly calculate the transition energy for the N−H σ * component as too large and that this component is thus buried in the main edge of the spectrum instead of contributing to the pre-edge [see the x (N−H) component and its shift for NMA in DMSO and acetone in Figure 3e].

In Supporting Information, we present a comparison of HCH/DFT calculations in different codes and also TDDFT calculations, none of which give an appreciable pre-edge shift. However, simulations with alternative high-level quantum chemical methods would be required to assert that the spectrum simulations are reliable. Even though we have a rough agreement in the simulation of the IR spectra, the evidence is not strong enough to assert that the MD simulations are fully realistic. We notice, however, that DFT-based spectrum simulations in combination with sampling over MD configurations have failed to produce a well-defined XAS pre-edge also in other systems.

CONCLUSIONS AND SUMMARY

In a combined IR and soft-X-ray absorption spectroscopic study we have investigated the hydrogen bonding interactions of *N*-methylaniline (NMA) with dimethyl sulfoxide (DMSO) and with acetone. The N−H stretching mode of NMA is a direct local probe for hydrogen bond geometries, even though disentangling the relative contributions due to the intrinsic hydrogen bond interaction of the NMA−solvent complex and those of the polar solvent shells with the complex are not straightforwardly done. However, N−H stretching frequency shifts experimentally measured and calculated using ab initio MD simulations are in good correspondence with each other, and calculated N−H···O distances are in line with the semiempirical correlations.[6]

The measured and calculated N−K edge spectra of NMA in DMSO or acetone show a proper correspondence in pre-edge and main-edge features. In particular, the calculations show that the pre-edge peak consists of transitions from the N 1s to the N_{LP} π^* and N−H σ^* antibonding orbitals. A decrease in hydrogen bond strength is reflected by a relative increase of the N−H σ^* component as well as a N_{LP} π^* frequency shift. Following the spectral response of this pre-edge peak during the breaking of the hydrogen bond suggests that the pre-edge peak spectral characteristic provides insight into the hydrogen bond geometries. However, a close inspection of the exact frequency shift of the pre-edge peaks in experiment and in the calculations suggests that further improvements of the XAS modeling is a necessary task for further substantiation of the current approach of hydrogen bonding of organic molecules in nonaqueous media.

ASSOCIATED CONTENT

Supporting Information

Supporting text and figures including details of calculations and calculated infrared absorption spectra. The Supporting Information is available free of charge on the ACS Publications website at DOI: 10.1021/acs.jpcb.5b02954.

AUTHOR INFORMATION

Corresponding Authors

*Phone: +49 30 63921477. Fax: +49 30 63921409. E-mail: nibberin@mbi-berlin.de.

*Phone: +46-8-5537 8713. Fax: +46-8-5537 8601. E-mail: odelius@fysik.su.se.

*Phone: +49 30 806213448. Fax: +49 30 806212114. E-mail: wernet@helmholtz-berlin.de.

Author Contributions

The manuscript was written through contributions of all authors. All authors have given approval to the final version of the manuscript.

Notes

The authors declare no competing financial interest.

ACKNOWLEDGMENTS

We thank HZB for the allocation of synchrotron radiation beamtime and the HZB staff for continuous support. We thank in particular Christian Weniger for making available the SiN membranes. M.O. acknowledges support from the Swedish Research Council, Carl Tryggers Foundation, and Magnus Bergvall Foundation. The theoretical modeling was made possible through generous allocations of computer time provided by the Swedish National Infrastructure for Computing (SNIC) at the Swedish National Supercomputer Center (NSC) and the High Performance Computer Center North (HPC2N) and Chalmers Centre for Computational Science and Engineering (C3SE), Sweden. E.T.J.N. is grateful for financial support from the German Science Foundation (DFG NI 492/11.1).

REFERENCES

(1) Watson, J. D.; Crick, F. H. C. Molecular Structure of Nucleic Acids - A Structure for Deoxyribose Nucleic Acid. *Nature* **1953**, *171*, 737−738.

(2) Saenger, W. *Principles of Nucleic Acid Structure*; Springer: New York, 1984.

(3) Franks, F. *Water, a Comprehensive Treatise*; Plenum: New York, 1972.

(4) Ohmine, I.; Saito, S. Water Dynamics: Fluctuation, Relaxation, and Chemical Reactions in Hydrogen Bond Network Rearrangement. *Acc. Chem. Res.* **1999**, *32*, 741−749.

(5) Novak, A. Hydrogen Bonding in Solids. Correlation of Spectroscopic and Crystallographic Data. *Struct. Bonding (Berlin, Ger.)* **1974**, *18*, 177−216.

(6) Lautié, A.; Froment, F.; Novak, A. Relationship between NH Stretching Frequencies and N···O Distances of Crystals Containing NH···O Hydrogen Bonds. *Spectrosc. Lett.* **1976**, *9*, 289−299.

(7) Mikenda, W. Stretching Frequency Versus Bond Distance Correlation of O—D(H)···Y (Y= N, O, S, Se, Cl, Br, I) Hydrogen Bonds in Solid Hydrates. *J. Mol. Struct.* **1986**, *147*, 1−15.

(8) Mikenda, W.; Steinböck, S. Stretching Frequency Vs. Bond Distance Correlation of Hydrogen Bonds in Solid Hydrates: A Generalized Correlation Function. *J. Mol. Struct.* **1996**, *384*, 159−163.

(9) Libowitzky, E. Correlation of O-H Stretching Frequencies and O-H···O Hydrogen Bond Lengths in Minerals. *Monatsh. Chem.* **1999**, *130*, 1047−1059.

(10) Ji, M.; Odelius, M.; Gaffney, K. Large Angular Jump Mechanism Observed for Hydrogen Bond Exchange in Aqueous Perchlorate Solution. *Science* **2010**, *328*, 1003−1005.

(11) Laage, D.; Hynes, J. T. A Molecular Jump Mechanism of Water Reorientation. *Science* **2006**, *311*, 832−835.

(12) Hadži, D.; Bratos, S. Vibrational Spectroscopy of the Hydrogen Bond. In *The Hydrogen Bond: Recent Developments in Theory and Experiments*; Schuster, P.; Zundel, G.; Sandorfy, C., Eds.; Amsterdam,

DOI: 10.1021/acs.jpcb.5b02954
J. Phys. Chem. B 2015, 119, 8115−8124

the Netherlands: North Holland, 1976; Vol. *II*, Structure and Spectroscopy, pp 565−611.
(13) Robertson, W. H.; Johnson, M. A. Molecular Aspects of Halide Ion Hydration: The Cluster Approach. *Annu. Rev. Phys. Chem.* **2003**, *54*, 173−213.
(14) Nibbering, E. T. J.; Elsaesser, T. Ultrafast Vibrational Dynamics of Hydrogen Bonds in the Condensed Phase. *Chem. Rev.* **2004**, *104*, 1887−1914.
(15) Headrick, J. M.; Diken, E. G.; Walters, R. S.; Hammer, N. I.; Christie, R. A.; Cui, J.; Myshakin, E. M.; Duncan, M. A.; Johnson, M. A.; Jordan, K. D. Spectral Signatures of Hydrated Proton Vibrations in Water Clusters. *Science* **2005**, *308*, 1765−1769.
(16) Bakker, H. J.; Skinner, J. L. Vibrational Spectroscopy as a Probe of Structure and Dynamics in Liquid Water. *Chem. Rev.* **2010**, *110*, 1498−1517.
(17) Skinner, J. L.; Auer, B. M.; Lin, Y. S. Vibrational Line Shapes, Spectral Diffusion, and Hydrogen Bonding in Liquid Water. *Adv. Chem. Phys.* **2009**, *142*, 59−103.
(18) Laage, D.; Stirnemann, G.; Sterpone, F.; Rey, R.; Hynes, J. T. Reorientation and Allied Dynamics in Water and Aqueous Solutions. *Annu. Rev. Phys. Chem.* **2011**, *62*, 395−416.
(19) Kiefer, P. M.; Hynes, J. T. Theoretical Aspects of Tunneling Proton Transfer Reactions in a Polar Environment. *J. Phys. Org. Chem.* **2010**, *23*, 632−646.
(20) Prémont-Schwarz, M.; Xiao, D. Q.; Batista, V. S.; Nibbering, E. T. J. The O−H Stretching Mode of a Prototypical Photoacid as a Local Dielectric Probe. *J. Phys. Chem. A* **2011**, *115*, 10511−10516.
(21) Xiao, D.; Prémont-Schwarz, M.; Nibbering, E. T. J.; Batista, V. S. Ultrafast Vibrational Frequency Shifts Induced by Electronic Excitations: Naphthols in Low Dielectric Media. *J. Phys. Chem. A* **2012**, *116*, 2775−2790.
(22) Stöhr, J. *NEXAFS Spectroscopy*; Springer: Berlin, 1992.
(23) Aria, H.; Horikawa, Y.; Sadakane, K.; Tokushima, T.; Harada, Y.; Senba, Y.; Ohashi, H.; Takata, Y.; Shin, S. Hydrogen Bonding of Water in 3-Methylpyridine Studied by O 1s X-ray Emission and Absorption Spectroscopy. *Phys. Chem. Chem. Phys.* **2012**, *14*, 1576−1580.
(24) Lange, K.; Hodeck, K.; Schade, U.; Aziz, E.. F. Nature of the Hydrogen Bond in Solvents of Different Polarities. *J. Phys. Chem. B* **2010**, *114*, 16997−17001.
(25) Wernet, Ph.; Nordlund, D.; Bergmann, U.; Ogasawara, H.; Cavalleri, M.; Näslund, L.-Å.; Hirsch, T.; Ojamäe, L.; Glatzel, P.; Odelius, M.; et al. The Structure of the First Coordination Shell in Liquid Water. *Science* **2004**, *304*, 995−999.
(26) Nilsson, A.; Nordlund, D.; Waluyo, I.; Huang, N.; Ogasawara, H.; Kaya, S.; Bergmann, U.; Näslund, L.-Å.; Öström, H.; Wernet, Ph; et al. X-ray Absorption Spectroscopy and X-ray Raman Scattering of Water and Ice; an Experimental View. *J. Electron Spectrosc. Relat. Phenom.* **2010**, *177*, 99−129.
(27) Nilsson, A.; Pettersson, L. G. M. Perspective on the Structure of Liquid Water. *Chem. Phys.* **2011**, *389*, 1−34.
(28) Huse, N.; Wen, H.; Nordlund, D.; Szilagyi, E.; Daranciang, D.; Miller, T. A.; Nilsson, A.; Schoenlein, R. W.; Lindenberg, A. M. Probing the Hydrogen-Bond Network of Water via Time-Resolved Soft X-ray Spectroscopy. *Phys. Chem. Chem. Phys.* **2009**, *11*, 3951−3957.
(29) Wernet, Ph.; Gavrila, G.; Godehusen, K.; Weniger, C.; Nibbering, E.; Elsaesser, T.; Eberhardt, W. Ultrafast Temperature Jump in Liquid Water Studied by a Novel Infrared Pump-x-ray Probe Technique. *Appl. Phys. A: Mater. Sci. Process.* **2008**, *92*, 511−516.
(30) Sellberg, J. A.; Kaya, S.; Segtnan, V. H.; Chen, C.; Tyliszczak, T.; Ogasawara, H.; Nordlund, D.; Pettersson, L. G. M.; Nilsson, A. Comparison of X-ray Absorption Spectra Between Water and Ice: New Ice Data With Low Pre-edge Absorption Cross-Section. *J. Chem. Phys.* **2014**, *141*, 034507.
(31) Nagasaka, M.; Mochizuki, K.; Leloup, V.; Kosugi, N. Local Structures of Methanol−Water Binary Solutions Studied by Soft X-ray Absorption Spectroscopy. *J. Phys. Chem. B* **2014**, *118*, 4388−4396.
(32) Ito, E.; Oji, E.; Araki, T.; Oichi, K.; Ishii, H.; Ouchi, Y.; Ohta, T.; Kosugi, N.; Maruyama, Y.; Naito, T.; et al. Soft X-ray Absorption and X-ray Photoelectron Spectroscopic Study of Tautomerism in Intramolecular Hydrogen Bonds of *N*-Salicylidenaniline Derivatives. *J. Am. Chem. Soc.* **1997**, *119*, 6336−6344.
(33) Horikawa, Y.; Arai, A.; Tokushima, T.; Shin, S. Spectral Fingerprint in X-ray Absorption for Hydrogen-Bonded Dimer Formation of Acetic Acids in Solution. *Chem. Phys. Lett.* **2012**, *522*, 33−37.
(34) Li, H.; Hua, W.; Lin, Z.; Luo, Y. First-Principles Study on Core-Level Spectroscopy of Arginine in Gas and Solid Phases. *J. Phys. Chem. B* **2012**, *116*, 12641−12650.
(35) Messer, B. M.; Cappa, C. D.; Smith, J. D.; Drisdell, W. S.; Schwartz, C. P.; Cohen, R. C.; Saykally, R. J. Local Hydration Environment of Amino Acids and Dipeptides Studied by X-ray Spectroscopy of Liquid Microjets. *J. Phys. Chem. B* **2005**, *109*, 21640−21646.
(36) Messer, B. M.; Cappa, C. D.; Smith, J. D.; Wilson, K. R.; Gilles, M. K.; Cohen, R. C.; Saykally, R. J. pH Dependence of the Electronic Structure of Glycine. *J. Phys. Chem. B* **2005**, *109*, 5375−5382.
(37) Hua, W.; Gao, B.; Li, S.; Agren, H.; Luo, Y. Refinement of DNA Structures through Near-Edge X-ray Absorption Fine Structure Analysis: Applications on Guanine and Cytosine Nucleobases, Nucleosides, and Nucleotides. *J. Phys. Chem. B* **2010**, *114*, 13214−13222.
(38) Schwartz, C. P.; Uejio, J. S.; Duffin, A. M.; England, A. H.; Predergast, D.; Saykally, R. J. Auto-oglomerization and Hydration of Pyrrole Revealed by X-ray Absorption Spectroscopy. *J. Chem. Phys.* **2009**, *131*, 114509.
(39) Schwartz, C. P.; Uejio, J. S.; Duffin, A. M.; England, A. H.; Kelly, D. N.; Predergast, D.; Saykally, R. J. Investigation of Protein Conformation and Interactions with Salts via X-ray Absorption Spectroscopy. *Proc. Nat. Acad. Sci. U. S. A.* **2011**, *108*, 20850.
(40) Greve, C.; Nibbering, E. T. J.; Fidder, H. Hydrogen-Bonding-Induced Enhancement of Fermi Resonances: A Linear IR and Nonlinear 2D-IR Study of Aniline-d_5. *J. Phys. Chem. B* **2013**, *117*, 15843−15855.
(41) Huang, N.; Nordlund, D.; Huang, C.; Bergmann, U.; Weiss, T. M.; Pettersson, L. G. M.; Nilsson, A. X-ray Raman Scattering Provides Evidence for Interfacial Acetonitrile−Water Dipole Interactions in Aqueous Solutions. *J. Chem. Phys.* **2011**, *135*, 164509.
(42) Lange, K.; Könnecke, R.; Soldatov, M.; Golnak, R.; Rubensson, J.-E.; Soldatov, A.; Aziz, E. F. On the Origin of the Hydrogen-Bond Network of Water: X-ray Absorption and Emission Spectra of Water-Acetonitrile Mixtures. *Angew. Chem., Int. Ed.* **2011**, *50*, 10621−10625.
(43) Engel, E.; Atak, K.; Lange, K.; Gotz, M.; Soldatov, M.; Golnak, R.; Suljoti, E.; Rubensson, J.-E.; Aziz, E. F. DMSO-Water Clustering in Solution Observed in Soft-x-ray Spectra. *J. Phys. Chem. Lett.* **2012**, *3*, 3697−3701.
(44) Uejio, J. S.; Schwartz, C. P.; Duffin, A. M.; England, A. H.; Predergast, D.; Saykally, R. J. Monopeptide versus Monopeptoid: Insights on Structure and Hydration of Aqueous Alanine and Sarcosine via X-ray Absorption Spectroscopy. *J. Phys. Chem. B* **2010**, *114*, 4702−4709.
(45) Lady, J. H.; Whetsel, K. B. Infrared Studies of Amine Complexes. I. Self-Association of Aniline in Cyclohexane Solution. *J. Phys. Chem.* **1964**, *68*, 1001−1009.
(46) Schreck, S.; Gavrila, G.; Weniger, C.; Wernet, Ph. A Sample Holder for Soft X-ray Absorption Spectroscopy of Liquids in Transmission Mode. *Rev. Sci. Instrum.* **2011**, *82*, 103101:1−10.
(47) Meibohm, J.; Schreck, S.; Wernet, Ph. Temperature Dependent Soft X-ray Absorption Spectroscopy of Liquids. *Rev. Sci. Instrum.* **2014**, *85*, 103102:1−7.
(48) Car, R.; Parrinello, M. Unified Approach for Molecular Dynamics and Density-Functional Theory. *Phys. Rev. Lett.* **1985**, *55*, 2471−2474.
(49) Lyubartsev, A. P.; Laaksonen, A. M. DynaMix - A Scalable Portable Parallel MD Simulation Package for Arbitrary Molecular Mixtures. *Comput. Phys. Commun.* **2000**, *128*, 565−589.
(50) Cornell, W. D.; Cieplak, P.; Bayly, C. I.; Gould, I. R.; Merz, K. M.; Ferguson, D. M.; Spellmeyer, D. C.; Fox, T.; Caldwell, J. W.;

DOI: 10.1021/acs.jpcb.5b02954
J. Phys. Chem. B 2015, 119, 8115−8124

Kollman, P. A. A Second Generation Force Field for the Simulation of Proteins, Nucleic Acids, and Organic Molecules. *J. Am. Chem. Soc.* **1995**, *117*, 5179−5197.
(51) Frisch, M. J.; Trucks, G. W.; Schlegel, H. B.; Scuseria, G. E.; Robb, M. A.; Cheeseman, J. R.; Scalmani, G.; Barone, V.; Mennucci, B.; Petersson, G. A.; et al. *Gaussian 09, Revision C.01*; Gaussian, Inc., Wallingford, CT, 2009.
(52) Becke, A. D. Density-Functional Thermochemistry. 3. The Role of Exact Exchange. *J. Chem. Phys.* **1993**, *98*, 5648−5652.
(53) Dunning, T. H., Jr. Gaussian Basis Sets for Use in Correlated Molecular Calculations. I. The Atoms Boron through Neon and Hydrogen. *J. Chem. Phys.* **1989**, *90*, 1007−23.
(54) Geerke, D. P.; Oostenbrink, C.; van der Vegt, N. F. A.; van Gunsteren, W. F. An Effective Force Field for Molecular Dynamics Simulations of Dimethyl Sulfoxide and Dimethyl Sulfoxide-Water Mixtures. *J. Phys. Chem. B* **2004**, *108*, 1436−1445.
(55) Jorgensen, W.; Maxwell, D.; Tirado-Rives, J. Development and Testing of the OPLS All-Atom Force Field on Conformational Energetics and Properties of Organic Liquids. *J. Am. Chem. Soc.* **1996**, *118*, 11225−11236.
(56) CPMD, http://www.cpmd.org/, copyright IBM Corp. 1990−2008, copyright MPI für Festkörperforschung Stuttgart 1997−2001.
(57) Becke, A. D. Density-Functional Exchange-Energy Approxiation with Correct Asymptotic Behavior. *Phys. Rev. A* **1988**, *38*, 3098−3100.
(58) Lee, C.; Yang, W.; Parr, R. G. Development of the Colle-Salvetti Correlation-Energy Formula into a Functional of the Electron Density. *Phys. Rev. B* **1988**, *37*, 785−789.
(59) Grimme, S. Semiempirical GGA-Type Density Functional Constructed with a Long-Range Dispersion Correction. *J. Comput. Chem.* **2006**, *27*, 1787−1799.
(60) Troullier, N.; Martins, J. L. Efficient Pseudopotentials for Plane-Wave Calculations. *Phys. Rev. B* **1991**, *43*, 1993−2006.
(61) Kleinman, L.; Bylander, D. M. Efficacious Form for Model Pseudopotentials. *Phys. Rev. Lett.* **1982**, *48*, 1425−1428.
(62) The CP2K Developers Group. Available at: http://www.cp2k.org/(2014).
(63) Hutter, J.; Iannuzzi, M.; Schiffmann, F.; VandeVondele, J. CP2K: Atomistic Simulations of Condensed Matter Systems. *Wiley Interdiscip. Rev.: Comput. Mol. Sci.* **2014**, *4*, 15−25.
(64) Iannuzzi, M.; Hutter, J. Inner-Shell Spectroscopy by the Gaussian and Augmented Plane Wave Method. *Phys. Chem. Chem. Phys.* **2007**, *9*, 1599−1610.
(65) Krack, M. Pseudopotentials for H to Kr Optimized for Gradient-Corrected Exchange-Correlation Functionals. *Theor. Chem. Acc.* **2005**, *114*, 145−152.
(66) Schaefer, A.; Huber, C.; Ahlrichs, R. Fully Optimized Contracted Gaussian-Basis Sets of Triple Zeta Valence Quality for Atoms Li to Kr. *J. Chem. Phys.* **1994**, *100*, 5829−35.
(67) Dyall, L. K. Solvent Effects on Infrared Spectra of Anilines. V. Anilines with No Ortho Substituents. *Spectrochim. Acta, Part A* **1969**, *25A*, 1423−1435.
(68) Zhang, W.; Carravetta, V.; Plekan, O.; Feyer, V.; Richter, R.; Coreno, M.; Prince, K. C. Electronic Structure of Aromatic Amino Acids Studied by Soft X-ray Spectroscopy. *J. Chem. Phys.* **2009**, *131*, 035103.
(69) Duflot, D.; Hannay, C.; Flament, J.-P.; Hubin-Franskin, M.-J. Electronic Excitation of Gaseous Pyrrole and Pyrazole by Inner-Shell Electron Loss Spectroscopy. *J. Chem. Phys.* **1998**, *109*, 5308.
(70) Laage, D.; Hynes, J. T. On the Molecular Mechanism of Water Reorientation. *J. Phys. Chem. B* **2008**, *112*, 14230−14242.
(71) Psciuk, B. T.; Prémont-Schwarz, M.; Koeppe, B.; Keinan, S.; Xiao, D.; Nibbering, E. T. J.; Batista, V. S. The O−H Stretching Mode of Aromatic Alcohols as an Ultrafast Local Probe of Photoacidity in Hydrogen-Bonded Complexes, *J. Phys. Chem. A*, appeared online, ASAP article, DOI: 10.1021/acs.jpca.5b01530.

DOI: 10.1021/acs.jpcb.5b02954
J. Phys. Chem. B 2015, 119, 8115−8124